

# Modeling and optical absorption of $\text{PbWO}_4$ single crystal doped with $\text{Cr}^{3+}$

Maroj Bharati <sup>a</sup>, Vikram Singh <sup>a</sup>, Ram Kripal <sup>b</sup>

<sup>a</sup>Department of Physics, Nehru Gram Bharti (DU), Jamunipur, Prayagraj, India

<sup>b</sup>EPR Laboratory, Department of Physics, University of Allahabad, Prayagraj-211002, India

---

## Abstract

Crystal field parameters of  $\text{Cr}^{3+}$  doped  $\text{PbWO}_4$  single crystal are obtained using superposition model. The zero field splitting parameter  $D$  is then estimated with the help of microscopic spin Hamiltonian theory. The theoretical zero field splitting parameter for  $\text{Cr}^{3+}$  in  $\text{PbWO}_4$  single crystal at tetragonal symmetry site is in good match with the experimental value. The local distortion is taken into account to find the crystal field parameters.

**Keywords:** A. Inorganic compounds; D. Crystal fields; D. Optical properties; D. Electron paramagnetic resonance.

---

Date of Submission: 12-07-2025

Date of acceptance: 24-07-2025

---

## I. Introduction

Electron paramagnetic resonance (EPR) gives information about the site location, local site symmetry, ground-state energy levels and zero field splitting (ZFS) parameters of transition ions doped in crystals [1, 2]. It also identifies the defects responsible for the charge compensation in the system.  $\text{Cr}^{3+}$  is one of the most studied transition metal ions with  $3d^3$  electronic configurations and  $^4A_2$  ground state [3].

Because of the combined effect of crystal field and the spin-orbit coupling, the principal mechanism for the zero field splitting of the ground state of  $3d^3$  ions is the spin-orbit interaction from an admixture of higher energy levels [4]. The superposition model (SPM) is quite helpful in finding the crystal field parameters and spin Hamiltonian parameters for various  $3d^n$  ions [5, 6].

Lead-tungstate ( $\text{PbWO}_4$ ) single crystals have become of increasing interest in recent years as promising scintillation crystals for electromagnetic calorimeters in high-energy physics because of their physicochemical properties, like high density, nonhygroscopicity, low radiation length, small Moliere radius, high efficiency for detecting ionizing radiations, fast response, sufficient radiation hardness, and low production cost [7-11]. It is the first choice for detector material in the large hadron collider (LHC) at CERN [12, 13].  $\text{PbWO}_4$  can also be used in positron emission tomography (PET) for medical diagnosis [14].

$\text{PbWO}_4$  has been doped with a wide variety of impurity ions in an effort to alter its scintillation properties. Heavy doping with trivalent ions, such as  $\text{Gd}^{3+}$  (or  $\text{La}^{3+}$ ), reduces the scintillation light intensity to a level lower than the Cherenkov light intensity [15]. The green emission of  $\text{PbWO}_4$  is closely related to structural defects [16]. Some luminescences are related to oxygen vacancies [17] and F-centers [9]. EPR can help in understanding the real lattice structure of  $\text{PbWO}_4$  and the importance of different lattice defects for scintillation processes in the material [18].

The EPR spectra of  $\text{Cr}^{3+}$  ions in  $\text{PbWO}_4$  single crystals were analyzed using an effective spin Hamiltonian [19]. The observed experimental resonance spectra were used to calculate the second-order zero-field splitting (ZFS) tensor and the spectroscopic splitting tensor  $g$ . The local site symmetry surrounding the  $\text{Cr}^{3+}$  ion was determined to be tetragonal based on the rotation patterns (at 10 K) and the ZFS parameters of the  $\text{Cr}^{3+}$  ion. For the  $\text{Cr}^{3+}$  ion, the ground state energy levels were computed. Instead of replacing the  $\text{W}^{6+}$  ions in oxygen tetrahedra, it was discovered that the  $\text{Cr}^{3+}$  ions in  $\text{PbWO}_4$  crystal replaced the  $\text{Pb}^{2+}$  ions in oxygen octahedra without nearby charge compensation. The absorption spectrum of  $\text{PbWO}_4$ :  $\text{Cr}^{3+}$  crystals is also measured [20]. The crystal-field theory has been used to calculate and assign the spectrum of the d-d transitions of  $\text{Cr}^{3+}$  ions in  $\text{PbWO}_4$  crystals with tetragonal symmetry. With  $T_d$  symmetry, the  $\text{Cr}^{3+}$  ion's ground state is  $^4T_1(^4F)$ . The  $\text{Cr}^{3+}$  ion in  $\text{PbWO}_4$  has tetragonal local symmetry. A tetragonal crystal field splits  $^4T_1(^4F)$  into  $^4A(^4T_1, ^4F)$  and  $^4E(^4T_1, ^4F)$  states in  $S_4$  symmetry.

In this work, crystal field parameters derived from the superposition model and perturbation equation are used to estimate the ZFS parameter  $D$  for the  $\text{Cr}^{3+}$  ion in  $\text{PbWO}_4$ . The ZFS parameter  $D$  thus evaluated matches well with the experimental value. In addition, CF energy bands are also calculated and compared with the experimental ones.

## II. Crystal Structure

Lead-tungstate,  $\text{PbWO}_4$ , crystals (occur in nature as tetragonal stolzite) crystallized with a scheelite type structure, space group  $I4_1/a$  [19, 21] with lattice parameters  $a = 0.5455$  nm and  $c = 1.2027$  nm at room temperature. The unit cell of the  $\text{PbWO}_4$  crystal contains four molecules. Eight oxygen atoms, which are part of  $\text{WO}_4$  tetrahedra, encircle each Pb ion. One W and four O atoms form a tetrahedron with  $aD_{2d}$  symmetry in a scheelite-type structure. The crystal structure of  $\text{PbWO}_4$  is depicted in Fig. 1.

The crystallographic axis system CAS ( $a, b, c$ ) is taken as shown in Fig. 1. A common axis system ( $a||x, b||y, c||z$ ) is taken to simplify the calculations.

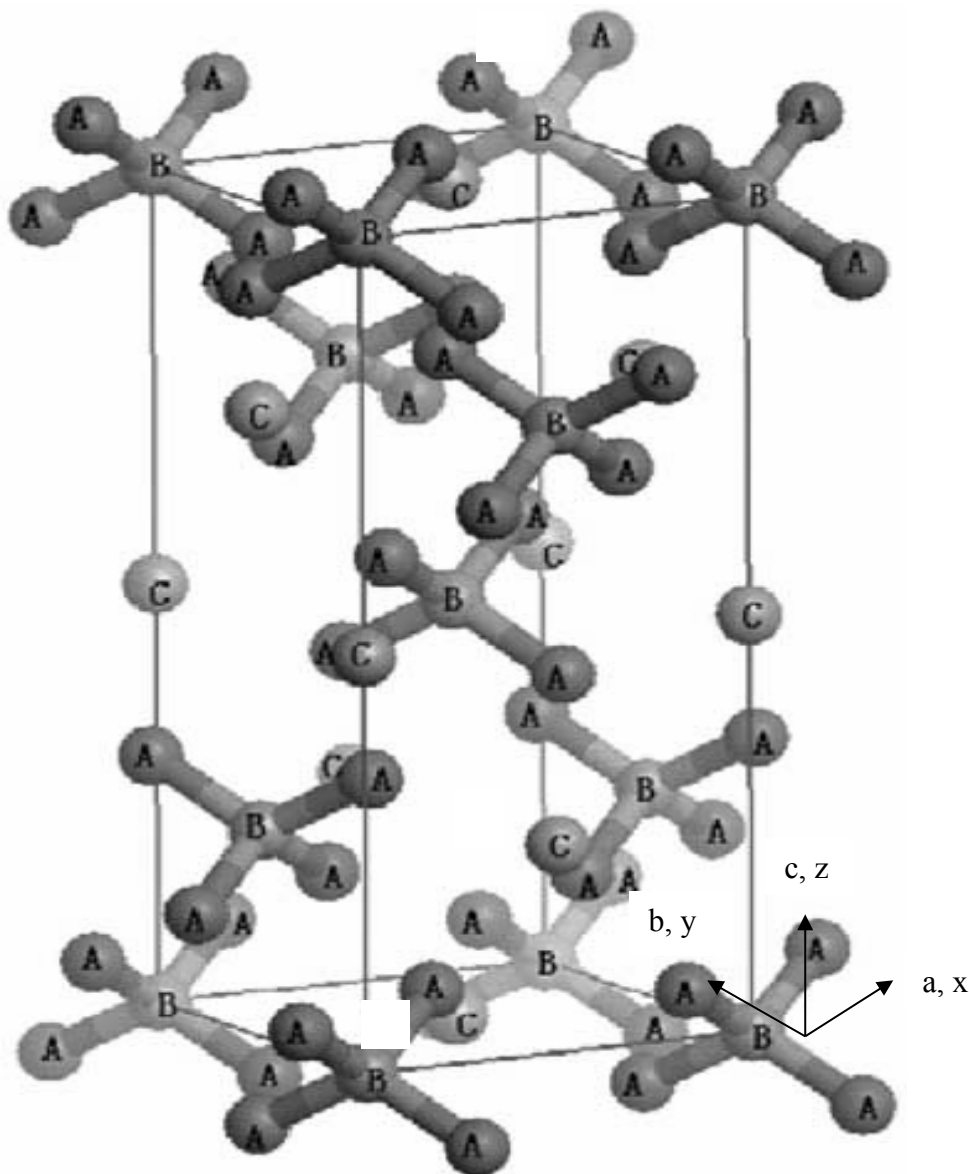


Fig. 1. (A) O, (B) W, and (C) Pb make up the crystal structure of the tetragonal lead tungstate,  $\text{PbWO}_4$ .

## III. Theoretical aspect

The ZFS parameter of  $\text{Cr}^{3+}$  ion is obtained using the microscopic spin Hamiltonian (MSH) theory [22]. Taking the ZFS and Zeeman terms, the effective spin Hamiltonian for  $\text{Cr}^{3+}$  ions at axial symmetry is given by [5].

$$= D \left\{ S_z^2 - \frac{1}{3} S(S+1) \right\} + \mu_B g_{\parallel} B_z S_z + \mu_B g_{\perp} (B_x S_x + B_y S_y) \quad \dots \dots (1)$$

where  $g_{\parallel}$  and  $g_{\perp}$  are the spectroscopic splitting factors,  $\mu_B$  is the Bohr magneton,  $S$  is the electronic spin,  $B$  is the external magnetic field and  $D$  is the second rank axial ZFS parameter.

For a doped crystal, the crystal field is given as

$$c = \sum B_{kq} C_q^{(k)} \quad \dots\dots\dots (2)$$

where  $B_{kq}$  are the crystal-field parameters in Wybourne notation and  $C_q^{(k)}$  are the Wybourne spherical tensor operators.

In  $\text{PbWO}_4$  single crystal, the local symmetry around  $\text{Cr}^{3+}$  ions is tetragonal. In tetragonal symmetry, the ZFS parameter  $D$  is given by [5]

$$D = \frac{1}{2} \left[ \epsilon \left( \left| E'(^4F \downarrow ^4A \downarrow ^4B) \right\rangle \right) - \epsilon \left( \left| E''(^4F \downarrow ^4A \downarrow ^4B) \right\rangle \right) \right] \quad (3)$$

where  $^4F$  ground term of  $3d^3(\text{Cr}^{3+})$  ions in tetrahedral symmetry splits into  $^4A$ ,  $^4T_2$  and  $^4T_1$  states,  $^4A$  being the ground state, and not split in axial field, but its irreducible representation changed into  $^4B$ . Due to the combined action of the axial field and magnetic interactions,  $^4B$  will split further, and this is expressed by group theory as:  $B - D^{(3/2)} \rightarrow B - (E' \odot E'') \rightarrow E' \odot E''$ ; the value of splitting is  $2D$ , where  $D$  is ZFS parameter of ground state.

Diagonalization of full Hamiltonian matrices yields the energy levels and eigen- vectors in terms of  $B_{kq}$ ,  $B$ ,  $C$  and  $\xi$ ; where  $B_{kq}$  are defined above,  $B$  and  $C$  are Racah parameters giving electron-electron repulsion and  $\xi$  is the spin-orbit coupling parameter. In terms of average covalency parameter  $N$ , the Racah parameters [23-25] and spin-orbit coupling parameter can be written as

$$B = N^4 B_0, \quad C = N^4 C_0, \quad \xi = N^2 \xi_0 \quad \dots\dots\dots (4)$$

where  $B_0$  and  $C_0$  are Racah parameters for free ion and  $\xi_0$  is free ion spin orbit coupling parameter. For  $\text{Cr}^{3+}$  ion  $B_0 = 920 \text{ cm}^{-1}$ ,  $C_0 = 3330 \text{ cm}^{-1}$ ,  $\xi_0 = 240 \text{ cm}^{-1}$  are taken [20, 24, 25].

Taking the values of Racah parameters ( $B = 814 \text{ cm}^{-1}$ ,  $C = 2948 \text{ cm}^{-1}$ ) found from optical study of  $\text{Cr}^{3+}$  doped  $\text{PbWO}_4$  crystal [20, 26], the average covalency parameter  $N = 0.9699$  is obtained employing

$$N = \left[ \sqrt{\frac{B}{B_0}} + \sqrt{\frac{C}{C_0}} \right] / 2 \quad \dots\dots\dots (5)$$

#### IV. Results and discussion

The SPM yields the crystal field parameters [27, 28] as

$$\sum_j \bar{A}_k(R_j) K_{kq}(\theta_j, \phi_j) = B_{kq} \quad \dots\dots\dots (6)$$

where  $K_{kq}(\theta_j, \phi_j)$  is an explicit function of the angular position of the ligand called the co-ordination factor.  $\bar{A}_k(R_j)$ , the intrinsic parameter is given by

$$\bar{A}_k(R_0) \left( \frac{R_0}{R_j} \right)^{t_k} = \bar{A}_k(R_j) \quad \dots\dots\dots (7)$$

where  $R_j$  is the distance of the ligand from the  $d^n$  ion,  $t_k$  gives the power law exponent,  $\bar{A}_k(R_0)$  is the intrinsic parameter of the reference crystal and  $R_0$  is the reference distance. Using superposition model the relation between the local structure parameters and crystal field parameters are written as [5]

$$B_{20} = -2 \bar{A}_2 \left( \frac{R_0}{R_{10} + \Delta R_1} \right)^{t_2} - 4 \bar{A}_2 \left( \frac{R_0}{R_{20} + \Delta R_2} \right)^{t_2} \quad \dots\dots\dots (8)$$

$$B_{40} = 16 \bar{A}_4 \left( \frac{R_0}{R_{10} + \Delta R_1} \right)^{t_4} + 12 \bar{A}_4 \left( \frac{R_0}{R_{20} + \Delta R_2} \right)^{t_4} \quad \dots\dots\dots (9)$$

$$B_{44} = 2\sqrt{70} \bar{A}_4 \left( \frac{R_0}{R_{20} + \Delta R_2} \right)^{t_4} \quad \dots\dots\dots (10)$$

Here, the reference distance  $R_0$  is taken as 0.255 nm, which is slightly larger than the sum of ionic radii of  $\text{Cr}^{3+}$  ion (0.0615 nm) and  $\text{O}^{2-}$  ion (0.138 nm) [25]. Due to the incorporation of the impurity ion in the crystal, the local environment of the paramagnetic ion may be different to that of the host ion and the bond lengths will

change. The bond lengths may be expressed in terms of the distortion parameters  $\Delta R_1$  and  $\Delta R_2$ , i.e.  $R_1 = R_{10} + \Delta R_1$ ,  $R_2 = R_{20} + \Delta R_2$ .  $\overline{A}_k$  and  $t_k$  are defined above. For tetrahedral coordination  $\overline{A}_4$  is represented as [29]

$$\overline{A}_4(R_0) = -\frac{27}{16}Dq \quad \dots\dots (11)$$

Using optical study [20, 26],  $Dq = 966 \text{ cm}^{-1}$  and so the value of  $\overline{A}_4(R_0) = 1630.13 \text{ cm}^{-1}$ . It is noted that the ratio  $\frac{\overline{A}_2(R_0)}{\overline{A}_4(R_0)}$  of  $\overline{A}_2$  and  $\overline{A}_4$  lies between 8 to 12, [24, 30, 31]. In the current investigation,  $\frac{\overline{A}_2}{\overline{A}_4} = 10$ , this gives  $\overline{A}_2 = 16301.3 \text{ cm}^{-1}$ . The crystal field parameters  $B_{kq}$  of  $\text{Cr}^{3+}$  ion in  $\text{PbWO}_4$  are calculated by taking the parameters  $\overline{A}_2$  and  $\overline{A}_4$  as well as arrangement of chlorine atoms around  $\text{Cr}^{3+}$  ion having matched experimental ZFS parameter. For  $\text{Cr}^{3+}$  ion in  $\text{PbWO}_4$ , the parameters  $t_2 = 4$  and  $t_4 = 6$  have been used. When  $\text{Cr}^{3+}$  ion substitutes the  $\text{Pb}^{2+}$  ion, the position of transition ion  $\text{Cr}^{3+}$  and spherical coordinates of ligands are shown in Table 1. The ZFS parameter  $D$  of  $\text{Cr}^{3+}$  ion in  $\text{PbWO}_4$  crystal is calculated from the expression (3) [5]. The distortion parameters used are:  $\Delta R_1 = 0.336233 \text{ nm}$  and  $\Delta R_2 = 0.120000 \text{ nm}$  with  $R_{10} = 0.6202 \text{ nm}$  and  $R_{20} = 0.6476 \text{ nm}$  for center I. The distance  $R_{10}$  is the average of the  $\text{Cr}^{3+}\text{-O}^{2-}$  (1) and  $\text{Cr}^{3+}\text{-O}^{2-}$  (3) bond lengths and  $R_{20}$  is the average of the  $\text{Cr}^{3+}\text{-O}^{2-}$  (2) and  $\text{Cr}^{3+}\text{-O}^{2-}$  (4) bond lengths.

Table 1. Fractional position of  $\text{Cr}^{3+}$  ion along with spherical co-ordinates (R,  $\theta$ ,  $\phi$ ) of ligands in  $\text{PbWO}_4$  single crystal.

Position of $\text{Cr}^{3+}$ (Fractional)	Ligands	Spherical co-ordinates of ligands					
		x	y	z	R(nm)	$\theta^\circ$ (degree)	$\phi^\circ$
Site : Substitutional Pb (0, 0.25, 0.625)	O1	0.2388	0.1141	0.0429	0.7159	167.91	-29.64
	O2	-0.2388	-0.1141	0.0429	0.7393	161.25	56.74
	O3	0.2388	0.6141	0.2071	0.5559	154.70	56.74
	O4	-0.2388	0.3859	0.2071	0.5245	163.39	-29.64

The calculated crystal field parameters and ZFS parameter along with reference distance with distortion are presented in Table 2. The above parameters without distortion with the same reference distance are also given in Table 2. The ZFS parameter calculated using crystal field parameters from superposition model for center I without distortion is smaller than the experimental value [19]. The

Table 2. Crystal field (CF) parameters and zero field splitting (ZFS) parameter  $D$  of  $\text{Cr}^{3+}$  doped  $\text{PbWO}_4$  single crystal with and without distortion.

Crystal- field parameters ( $\text{cm}^{-1}$ )							Zero-field splitting parameter ( $10^{-4}\text{cm}^{-1}$ )
$\Delta R_1$ (nm)	$\Delta R_2$ (nm)	$R_0$ (nm)	$B_{20}$	$B_{40}$	$B_{44}$	$ D $	
I	0.336233	0.120000	0.255	-17636.5	13421.82	-347.717	862.8
	0.000000	0.000000	0.255	2499.158	-198.898	-101.674	1.8
						Exptl. [19]	862.8

ZFS parameter calculated employing crystal field parameters from superposition model for center I with distortion is in good agreement with the experimental value [19] as can be seen from Table 2. With the help of  $B_{kq}$  parameters and CFA program [32-33], the optical spectra of  $\text{Cr}^{3+}$  doped  $\text{PbWO}_4$  crystal are calculated. The energy levels of the impurity ion are computed by diagonalizing the complete Hamiltonian which consists of the Coulomb interaction (in terms of B and C parameters), Trees correction, the spin-orbit interaction, the crystal field Hamiltonian, the spin-spin interaction and the spin-other orbit interaction. The computed energy values are shown in Table 3 (input parameters are given below the Table) along with the experimental values [20] for comparison. It is noted from Table 3 that there is a reasonable match with the experimental energy values [20].

Table 3. Computed energy band positions of  $\text{Cr}^{3+}$  doped  $\text{PbWO}_4$  single crystal along with the experimental values for comparison.

Transition from $^4\text{A} (^4\text{T}_1, ^4\text{F})$	Observed energy bands ( $\text{cm}^{-1}$ )  [20]	Calculated energy bands ( $\text{cm}^{-1}$ ) With distortion I
$^4\text{E} (^4\text{T}_1, ^4\text{F})$		5962, 6046, 6122, 6192
$^4\text{E} (^4\text{T}_2, ^4\text{F})$		8392, 12199, 13360, 13941
$^4\text{B} (^4\text{T}_2, ^4\text{F})$	21368	20616, 20661
$^4\text{B} (^4\text{A}_2, ^4\text{F})$	23148	20742, 22927
$^4\text{E} (^4\text{T}_1, ^4\text{P})$	23584	22944, 23233, 23618, 24419
$^2\text{E}$	24753	24744, 25125
$^4\text{A} (^4\text{T}_1, ^4\text{P})$	28090	28340, 28573

Input parameters: Numbers of free ion parameters = 5, number of d shell electrons = 3, number of fold for rotational site symmetry = 1; Racah parameters in A, B and C, spin-orbit coupling constant and Trees correction are 0, 814, 2948, 240 and  $70 \text{ cm}^{-1}$ , respectively; number of crystal field parameters = 3;  $B_{20}$ ,  $B_{40}$ ,  $B_{44}$  are taken from Table 2, spin-spin interaction parameter,  $M0 = 0.0201$ ; spin-spin interaction parameter,  $M2 = 0.0159$ ; spin-other-orbit interaction parameter,  $M00 = 0.0201$ ; spin-other-orbit interaction parameter,  $M22 = 0.0159$ ; magnetic field,  $B = 0.0 \text{ Gauss}$ ; angle between magnetic field B and z-axis =  $0.00 \text{ degree}$ .

It is observed from Table 2 that considering a small lattice distortion gives good agreement between theoretical and experimental results. This suggests that the distortion model employed here is quite reasonable. The parameters  $\Delta R_1$  and  $\Delta R_2$  are negative, which shows that the bond length of Cr-O is smaller than Pb-O. When distortion in the crystal is neglected, a smaller value of D is obtained. Taking a small distortion, the calculated ZFS parameter D is very close to the experimental value. This indicates that local distortion has an important role in the contribution to ZFS parameter and therefore must be taken into account in the calculation.

## V. Conclusions:

$\text{Cr}^{3+}$  ions substitute at  $\text{Pb}^{2+}$  sites in  $\text{PbWO}_4$  crystal. The differences of charge and ionic radii between  $\text{Cr}^{3+}$  and  $\text{Pb}^{2+}$  ions provide local distortion around  $\text{Cr}^{3+}$  impurity. The theoretical investigation of ZFS parameter has been done using perturbation formula and crystal field parameters found from superposition model. Taking local distortion, the ZFS parameter values of  $\text{Cr}^{3+}$  ion in  $\text{PbWO}_4$  crystal for center I is in good agreement with the experimental values. It is also found that there is a reasonable agreement between the computed and experimental optical energy values. Thus the theoretical result supports the conclusion of the experimental study.

## Acknowledgement

The authors are thankful to the Head, Department of Physics for providing the facilities of the department and to Prof. C. Rudowicz, Faculty of Chemistry, Adam Mickiewicz University, Poznan, Poland for CFA program.

## Declarations

## Ethical Approval:

This research did not contain any studies involving animal or human participants, nor did it take place on any private or protected areas. No specific permissions were required for corresponding locations.

**Competing interests:**

The authors declare that they have no known competing financial interests or personal relationships that could have appeared to influence the work reported in this paper.

**Authors' contributions:**

Maroj Bharati and Vikram Singh- performed calculations, wrote the manuscript and prepared the figure.

Ram Kripal- idea and supervision.

All authors have reviewed the manuscript.

**Funding:**

No funding is received.

**Availability of data and materials:**

The data will be made available on request.

**References:**

- [1]. Z. Wen-Chen, W. Shao-Yi, D. Hui-Ning, Z. Jian, Spectrochim. Acta A 58(2002)537-541.
- [2]. J. A. Weil, J. R. Bolton, J. E. Wertz, Electron Paramagnetic Resonance: Elementary Theory and Practical Applications, Wiley, New York, 1994.
- [3]. Y. Y. Yeung, D. J. Newman, Phys. Rev. B 34(1986)2258-2265.
- [4]. C. Rudowicz, P. Gnutek, M. Açıkgoz, Appl. Spectroscopy Rev. 54(2019) 673-718.
- [5]. Q. Wei, Acta Phys. Polon. A 118(2010)670-672.
- [6]. M. G. Brik, N. M. Avram (Eds.), Optical Properties of 3d-Ions in Crystals: Spectroscopy and Crystal Field Analysis, Chapter 3, Springer, 2013, pp. 95-121.
- [7]. V. G. Baryshevsky, M. V. Korzhik, V. I. Moroz, V. B. Palvenko, A. F. Lobko, A. A. Fedorov, V. A. Kochanov, S. G. Solovyanov, D. N. Zadneprovskii, V. A. Nefedov, P. V. Dorogovin and L. L. Nagornaya, Nucl. Instr. Meth. Phys. Res. A 322 (1992) 231-234.
- [8]. M. Kobayashi, M. Ishii, Y. Usuki and H. Yahagi, Nucl. Instr. Meth. Phys. Res. A 333 (1993) 429-433.
- [9]. K. Nitsch, M. Nikl, S. Ganschow, P. Reiche and R. Uecker, J. Cryst. Growth 165 (1996) 163-165.
- [10]. M. Kobayashi, M. Ishii and Y. Usuki, Nucl. Instr. Meth. Phys. Res. A 406 (1998) 442-450.
- [11]. K. Hara, M. Ishii, M. Nikl, H. Takano, M. Tanaka, K. Tanji and Y. Ushki, Nucl. Instr. Meth. Phys. Res. A 414 (1998) 325-331.
- [12]. P. Lecoq, I. Dafinei, E. Auffray, M. Schneegans, M. V. Korzhik, O. V. Missevitch, V. B. Pavlenko, A. A. Fedorov, A. N. Annenkov, V. L. Kostylev, and V. D. Ligon, Nucl. Instrum. Meth. Phys. Res. A 365 (1995) 291-298.
- [13]. R. Y. Zhu, D. A. Ma, K. B. Newman, C. L. Woody, J. A. Kirstead, S. P. Stoll, and P. W. Levy, Nucl. Instrum. Meth. Phys. Res. A 376 (1996) 319-334.
- [14]. M. Kobayashi, Y. Usuki, M. Ishii and M. Nikl, Nucl. Instr. Meth. Phys. Res. A 486 (2002) 170-175.
- [15]. M. Kobayashi, Y. Usuki, M. Ishii, T. Yazawa, K. Hara, M. Tanaka, M. Nikl, S. Baccaro, A. Cecilia, M. Diemoz, I. Dafinei, Nucl. Instr. Meth. Phys. Res. A 404 (1998) 149-156.
- [16]. Z. Qi, C. Shi, D. Zhou, H. Tang, T. Liu and T. Hu, Physica B: Condens. Matter 307 (2001) 45-50.
- [17]. C. Shi, Y. Wei, X. Yang, D. Zhou, C. Guo, J. Liao and H. Tang, Chem. Phys. Lett. 328 (2000) 1-4.
- [18]. T. H. Yeom, S. H. Lee, S. H. Choh and D. Choi, J. Korean Phys. Soc. 32(9) (1998) 647-649.
- [19]. T. H. Yeom, S. H. Lee, I. G. Kim, S. H. Choh, T. H. Kim, J. H. Rao, J. Korean Phys. Soc. 44(6)(2004)1513-1517.
- [20]. D. Ergu, M. Du, H. Xie, T. H. Yeom, Phys. Stat. Sol. B234(2)(2002)660-664.
- [21]. J. M. Moreau, Ph. Galez, J. P. Pelgneux, M. V. Korzhik, J. Alloys Compds. 238(1996)46-48.
- [22]. C. Rudowicz, Magn. Reson. Rev. 13 (1987) 1-89.
- [23]. W. L. Yu, M. G. Zhao, J. Phys. C: Solid State Phys., 17(1984) L525-L527.
- [24]. A. Abragam, B. Bleaney, Electron Paramagnetic Resonance of Transition Ions, Clarendon Press, Oxford, 1970.
- [25]. C. K. Jorgensen, Modern Aspects of Ligand Field Theory, North-Holland, Amsterdam, 1971, p.305.
- [26]. Z. Min-Guang, X. Ji-An, B. Gui-Ru, X. Huong-Sen, Phys. Rev. B 27(3)(1983)1516-1522.
- [27]. W. L. Yu, M. G. Zhao, Phys. Rev. B 37 (1988) 9254-9267.
- [28]. D. J. Newman, B. Ng, Rep. Prog. Phys. 52(1989)699-763.
- [29]. D.J. Newman, B. Ng (Eds.), Crystal Field Handbook, Cambridge University Press, Cambridge, 2000.
- [30]. D. J. Newman, D. C. Pryce, W.A. Runciman, Am. Miner. 63 (1978) 1278-1281.
- [31]. T. H. Yeom, S. H. Choh, M. L. Du, J. Phys.: Condens. Matter 5 (1993) 2017-2024.
- [32]. Y. Y. Yeung, C. Rudowicz, J. Comput. Phys. 109(1993) 150-152.
- [33]. Y. Y. Yeung, C. Rudowicz, Comput. Chem. 16 (1992) 207-216.